

**CASE FILE  
COPY**

RM L52F24

NACA RM L52F24

**NACA**

# RESEARCH MEMORANDUM

CALIBRATION OF A COMBINED PITOT-STATIC TUBE AND  
VANE-TYPE FLOW ANGULARITY INDICATOR AT  
TRANSONIC SPEEDS AND AT LARGE ANGLES  
OF ATTACK OR YAW

By Albin O. Pearson and Harold A. Brown

Langley Aeronautical Laboratory  
Langley Field, Va.

**NATIONAL ADVISORY COMMITTEE  
FOR AERONAUTICS  
WASHINGTON**

September 17, 1952  
Declassified October 12, 1954

## NATIONAL ADVISORY COMMITTEE FOR AERONAUTICS

## RESEARCH MEMORANDUM

CALIBRATION OF A COMBINED PITOT-STATIC TUBE AND  
VANE-TYPE FLOW ANGULARITY INDICATOR AT  
TRANSONIC SPEEDS AND AT LARGE ANGLES  
OF ATTACK OR YAW

By Albin O. Pearson and Harold A. Brown

## SUMMARY

A wind-tunnel investigation has been made to provide information concerning the characteristics of a combined pitot-static tube and vane-type flow-angularity indicator at large angles of attack or yaw and at speeds near the speed of sound.

The results indicate that the angles of attack or yaw at which the total-pressure error is 0.01 (after correction of indicated total pressures for losses due to bow wave ahead of tube at Mach numbers greater than 1.00) vary linearly with Mach number and increase from approximately  $21.0^\circ$  at a Mach number of 0.60 to about  $24.3^\circ$  at a Mach number of 1.10. The static-pressure error is affected more by changes in angle of yaw than by corresponding changes in angle of attack and is positive (measured pressure greater than stream pressure) for angles of attack and negative for angles of yaw. The calibration factor for the pitot-static tube varies linearly with Mach number up to a Mach number of approximately 0.99 followed by an abrupt decrease in value at a Mach number near 1.00. The maximum error in measuring flow angularity by means of the vanes is of the order of  $1.5^\circ$  and occurs at a Mach number of 1.10 and an angle of attack of  $25^\circ$ .

## INTRODUCTION

Information concerning the total- and static-pressure errors of pitot-static tubes at large angles of attack or yaw and at speeds near the speed of sound is limited.

The present investigation was undertaken in the Langley 8-foot transonic tunnel to calibrate a pitot-static tube and vane-type flow-angularity indicator especially designed for use on transonic research aircraft and also to supplement existing data of pitot-static-tube pressure errors at large angles of attack or yaw and at speeds near the speed of sound. The results presented are for Mach numbers from about 0.60 to approximately 1.11, angles of attack from  $-10^\circ$  to  $25^\circ$ , and angles of yaw from  $-20^\circ$  to  $20^\circ$ .

## SYMBOLS

$H_o$	stream total pressure
$H_T$	total pressure indicated by instrument
$p_o$	stream static pressure
$p_T$	static pressure indicated by instrument
$q_c$	impact pressure, $H_o - p_o$
$\frac{\Delta H}{q_c}$	error in total pressure, $\frac{H_T - H_o}{H_o - p_o}$
$\frac{\Delta p}{q_c}$	error in static pressure, $\frac{p_T - p_o}{H_o - p_o}$
$\frac{H_o - p_o}{H_T - p_T}$	pitot-static-tube calibration factor
$M_o$	stream Mach number
$\alpha$	angle of attack
$\psi$	angle of yaw
$\alpha'$	angle of attack at which $\frac{\Delta H}{q_c} = 0.01$ ( $\Delta H$ corrected for loss due to bow wave at $M_o > 1.0$ )
$\psi'$	angle of yaw at which $\frac{\Delta H}{q_c} = 0.01$ ( $\Delta H$ corrected for loss due to bow wave at $M_o > 1.0$ )

## APPARATUS AND TESTS

The instrument which was calibrated in this investigation (fig. 1) consisted of a pitot-static tube for indicating total and static pressures and swiveling vanes for indicating the angularity of the tube with respect to the stream flow.

The pitot-static-tube component of the instrument consisted of an ogival-shaped forebody containing a sharp-edged total-pressure opening in its nose. A  $\frac{7}{8}$ -inch-diameter cylindrical afterbody contained static-pressure orifices located about  $8\frac{1}{2}$  inches downstream of the nose and  $12\frac{1}{4}$  inches upstream of the  $1\frac{5}{8}$ -inch-diameter enlargement. These static-pressure orifices were asymmetrically located in the upper and lower surfaces of the tube to reduce the static-pressure error at angle of attack. Details of both the total-pressure opening and the static-pressure orifices are given in figure 2.

The angularity-indicator component of the instrument consisted of swiveling vanes which were located well downstream of the static-pressure orifices (fig. 1) and each of which was mass-balanced about its axis of rotation. The angularity of the vanes (alined with the air stream) with respect to the tube was transmitted through linkages to synchro transmitters. The change of position of the synchro transmitter was measured by means of the displacement of a light trace on photographic film.

The method of mounting the instrument in the test section of the Langley 8-foot transonic tunnel involved the use of interchangeable bent support tubes attached to a remotely controlled sting-support system (see fig. 3). This support arrangement was designed to keep the static-pressure orifices near the axial center line of the tunnel and to permit testing at angles of as much as  $30^\circ$  from the flow direction. The 36-inch length of the bent support tubes permitted the location of the instrument static-pressure orifices well ahead of the sting enlargement.

The tests were performed by maintaining the tube at a constant angle and varying the stream Mach number. The tube was maintained at a constant angle by using the remotely controlled sting in conjunction with a cathetometer. The true angle of the instrument was obtained by measuring the angle of the tube before and after each test run with a sensitive inclinometer and correcting this measurement for an indicated upflow of approximately  $0.1^\circ$  in the model-free test-section flow (reference 1).

The stream total pressure was obtained from the measured total pressure in the low-speed section upstream of the tunnel contraction cone; a correction of approximately 0.4 lb/sq ft was applied to the measured total pressure in the low-speed section to compensate for a slight loss in total pressure between the low-speed and test sections.

The stream Mach number and stream static pressure were determined from simultaneously measured values of the stream total pressure and test chamber static pressure used in conjunction with calibration curves similar to those reported in reference 1.

Schlieren pictures were used in examining the static pressures indicated by the instrument for the effects of boundary disturbances.

#### PRECISION OF DATA

In the immediate vicinity of the instrument the magnitudes of maximum deviations in the tunnel calibration Mach number through the high-subsonic flow region were no greater than about 0.003, whereas those in the supersonic flow region were as much as 0.01.

The error in  $\Delta p/q_c$  was estimated to be less than 0.003 throughout the subsonic flow region and of the order of 0.01 in the supersonic flow region.

The possible error in  $\Delta H/q_c$  was estimated to range from a value of 0.003 at a Mach number of 0.60 to about 0.001 at a Mach number of 1.11.

The possible error in measuring the angularity of the pitot-static tube was estimated to be about  $0.1^\circ$ , whereas the error in determining the relative angularity between the vanes and the tube was of the order of  $0.3^\circ$ . This latter error was due mostly to difficulty in film reading caused by vane fluctuations, particularly at the larger angles when the vanes were in the wake of the pitot-static tube.

#### RESULTS AND DISCUSSION

##### Pitot-Static Tube

Total-pressure error.- The variation with Mach number of the total-pressure error for the instrument at various angles of attack ( $\psi = 0^\circ$ ) and yaw ( $\alpha = 0^\circ$ ) is shown in figures 4 and 5, respectively. These data indicate that in the subsonic flow region (from a Mach number of 0.60

to about 0.99) the total-pressure error for a given angle of attack or yaw remained constant except at the large angles ( $20^\circ$  and  $25^\circ$ ) where the error decreased with increase in Mach number. As the Mach number was further increased in the supersonic flow region the error increased (due to influence of bow wave) for all angles.

The variation of the total-pressure error with angles of attack ( $\psi = 0^\circ$ ) and yaw ( $\alpha = 0^\circ$ ) is shown in figures 6 and 7, respectively. These data indicate that the total-pressure error is essentially zero (after correction of indicated total pressures for losses due to bow wave ahead of tube at Mach numbers greater than 1.00) over an angular range of about  $\pm 15^\circ$  throughout the Mach number range (0.06 to 1.1, approximately) of this investigation. For angles of attack equal to or larger than about  $20^\circ$  the total pressures indicated by the instrument were significantly less than stream values. Although total-pressure data are not presented for angles of yaw greater than about  $20^\circ$ , it appears reasonable that they should be approximately the same as the angle-of-attack data presented.

The angle at which the total-pressure error is equal to 0.01 after correction of the indicated total pressures for losses due to bow wave at Mach numbers greater than 1.00 (a criterion used in refs. 2, 3, and 4) is shown to increase linearly with Mach number (fig. 8) from a value of approximately  $21.0^\circ$  at a Mach number of 0.60 to about  $24.3^\circ$  at a Mach number of 1.10. The data from the present investigation are shown to be consistent with those for a similar total-pressure tube E-5 reported in references 3 and 4 for stream Mach numbers of approximately 0.26 and 1.62, respectively.

Static-pressure error.- The variation with Mach number of static-pressure error for various angles of attack ( $\psi = 0^\circ$ ) and yaw ( $\alpha = 0^\circ$ ) is shown in figures 9 and 10, respectively.

The data of figure 9 ( $\psi = 0^\circ$ ) show that at an angle of attack of about  $0^\circ$  the static-pressure error is positive (measured pressure greater than stream pressure) and varies from approximately 0.004 at a Mach number of 0.60 to about 0.010 at a Mach number of 0.99, indicating that for subsonic flow the pressures at the orifices are affected by the presence of the tube enlargement downstream of the orifices. For Mach numbers greater than 1.00 the static-pressure error is essentially zero. For a given angle of attack other than  $0^\circ$  the static-pressure error remains nearly constant throughout the subsonic flow region except at the large angles ( $20^\circ$  and  $25^\circ$ ) and then becomes less positive in the supersonic flow region. The data of figure 10 ( $\alpha = 0^\circ$ ) show that for angles of yaw the variation of static-pressure error with Mach number is essentially linear and tends to decrease with increase in Mach number; data at corresponding positive and negative values of angle of yaw are essentially the same.

In the high-subsonic flow region (stream Mach numbers near 0.99 to 1.00) the data of figures 9 and 10 show a significant compressive effect caused by a bow wave (due to the enlarged portion of the tube downstream of the static-pressure orifices) in the vicinity of the static-pressure orifices (see fig. 11,  $M_0 = 1.000$ ).

At stream Mach numbers greater than 1.00 the experimental data show the effects of over-expansions and compressions due to boundary-reflected disturbances in the Mach-number ranges of 1.01 to 1.025 and 1.025 to 1.040, respectively. (See discussion of these boundary-reflected disturbances in ref. 1.) The compressions indicated at Mach numbers from about 1.07 to 1.09 are probably due to gradual disturbances (not visible in schlieren pictures) originating at the boundary.

Compensation for these latter disturbances could probably have been made if a more complete tunnel calibration were available throughout this Mach number range.

Although the various flow disturbances at stream Mach numbers greater than 1.00 produce variations in the indicated static-pressure error (figs. 9 and 10) approximate fairing of the experimental data can be estimated from knowledge of the direction of the variations and the Mach numbers at which they occur. Based upon this knowledge, the estimated fairing of the data yielded the values indicated by the broken lines of figures 9 and 10.

Schlieren pictures taken in conjunction with pressure measurements during a typical test run are presented in figure 11 to illustrate further the formation and movement of the shocks previously described. The static-pressure orifices are shown as white dots to aid in locating the various shock phenomena with respect to the orifices. The bow wave due to the enlargement of the tube downstream of the orifices is labeled (a) and the bow wave ahead of the nose of the tube, (b). In the high-subsonic flow region at Mach numbers of 0.977 and 0.995 weak normal shocks are formed at the static-pressure orifices. The bow wave (a) due to the enlargement of the tube downstream of the orifices may be seen at the left of the picture for a Mach number of 1.00. The following pictures illustrate the movement of this bow wave across the schlieren field of view until it finally assumes a position ahead of the enlargement, out of the schlieren view. The picture taken at a Mach number of 1.028 shows the reflection from the tunnel boundary of the bow wave (b) ahead of the instrument. This same reflected shock is also visible at a Mach number of 1.035 where it has moved farther downstream of the orifices. The remaining pictures indicate that the flow is relatively free of abrupt disturbances in the vicinity of the static orifices.

The effect of angle of attack on the static-pressure error is illustrated in figure 12. For all Mach numbers shown in this figure the

static-pressure error becomes more positive (measured pressure greater than stream pressure) with increasing angle of attack.

In the yaw direction the static-pressure error is negative and increases in magnitude as the angle is varied from  $0^\circ$  (fig. 13). The static-pressure error is affected more by changes in angle of yaw than by corresponding changes in angle of attack due to the asymmetric arrangement of the static-pressure orifices.

Calibration factor.- The calibration factors for the pitot-static tube are given in figures 14 and 15 for angles of attack and yaw, respectively. The plots shown in these figures are based on actual test data for Mach numbers less than 1.0. For Mach numbers greater than 1.0, total pressures are determined from the plots of figures 4 and 5 and static pressures from the estimated fairing of figures 9 and 10.

Since the total-pressure error is negligible at subsonic speeds through an angle-of-attack or yaw range from about  $-15^\circ$  to  $15^\circ$  the calibration factor in this angle range is affected only by the static-pressure error. The variation of the calibration factor within this angle range is therefore similar to the variation of the static-pressure error as can be seen by a comparison of figure 9 with figure 14 and of figure 10 with figure 15. Abrupt decreases in the calibration factor occur for all angles of attack or yaw at a Mach number near 1.00. For angles of attack the calibration factor varies from approximately 1.00 at an angle of  $-10^\circ$  to 1.07 at  $25^\circ$  in the subsonic flow region. In the supersonic flow region the minimum value of the calibration factor occurs at a Mach number of about 1.05 and varies from 0.99 at  $\alpha = -10^\circ$  to 1.03 at  $\alpha = 25^\circ$ . For angles of yaw the calibration factor varies from approximately 1.01 at an angle of  $0^\circ$  to 0.88 at an angle of  $\pm 20^\circ$  in the subsonic flow region and from 1.00 to 0.89 in the supersonic flow region.

#### Angularity Indicator

The correction curves for angle-of-attack and yaw measurements are shown in figure 16. These curves are linear from approximately  $-5^\circ$  to the maximum positive angle of this investigation. The maximum error in measuring the angularity of the tube with respect to the stream flow by means of the vanes is of the order of  $1.5^\circ$  and occurs at a Mach number of about 1.10 and an angle of attack of  $25^\circ$ .



## CONCLUDING REMARKS

Wind-tunnel calibration of a combination pitot-static tube and vane-type flow-angularity indicator at transonic speeds and at large angles of attack or yaw has indicated that:

1. The variation with Mach number of the angles of attack or yaw at which the total-pressure error is 0.01 (after correction of indicated total pressures for losses due to bow wave ahead of tube at Mach numbers greater than 1.00) is linear and increases from approximately  $21.0^\circ$  at a Mach number of 0.60 to about  $24.3^\circ$  at a Mach number of 1.10.

2. At an angle of attack of  $0^\circ$  the static-pressure error is positive (measured pressure greater than stream pressure) and varies linearly from approximately 0.4 percent of the stream impact pressure at a Mach number of 0.60 to about 1.0 percent of the stream impact pressure at a Mach number of 0.99 and then decreases to a value of zero in the supersonic flow region. For angles of attack the error becomes increasingly positive as the angle is increased above  $0^\circ$  whereas for angles of yaw the error becomes increasingly negative. The error is less for angles of attack than for corresponding angles of yaw due to the asymmetrical arrangement of the static-pressure orifices.

3. Variation of the calibration factor with Mach number is nearly linear up to a Mach number of about 0.99 followed by an abrupt decrease in value at a Mach number near 1.00.

4. The maximum error in angle measurement as determined from swiveling vanes is of the order of  $1.5^\circ$  and occurs at a Mach number of 1.10 and an angle of attack of  $25^\circ$ .

Langley Aeronautical Laboratory  
National Advisory Committee for Aeronautics  
Langley Field, Va.

## REFERENCES

1. Ritchie, Virgil S., and Pearson, Albin O.: Calibration of the Slotted Test Section of the Langley 8-Foot Transonic Tunnel and Preliminary Experimental Investigation of Boundary-Reflected Disturbances. NACA RM L51K14, 1952.
2. Gracey, William, Pearson, Albin O., and Russell, Walter R.: Wind-Tunnel Investigation of a Shielded Total-Pressure Tube at Transonic Speeds. NACA RM L51K19, 1952.
3. Gracey, William, Coletti, Donald E., and Russell, Walter R.: Wind-Tunnel Investigation of a Number of Total-Pressure Tubes at High Angles of Attack. Supersonic Speeds. NACA TN 2261, 1951.
4. Gracey, William, Letko, William, and Russell, Walter R.: Wind-Tunnel Investigation of a Number of Total-Pressure Tubes at High Angles of Attack. Subsonic Speeds. NACA TN 2331, 1951. (Supersedes NACA RM L50G19.)
5. Wright, Ray H., and Ritchie, Virgil S.: Characteristics of a Transonic Test Section With Various Slot Shapes in the Langley 8-Foot High-Speed Tunnel. NACA RM L51H10, 1951.

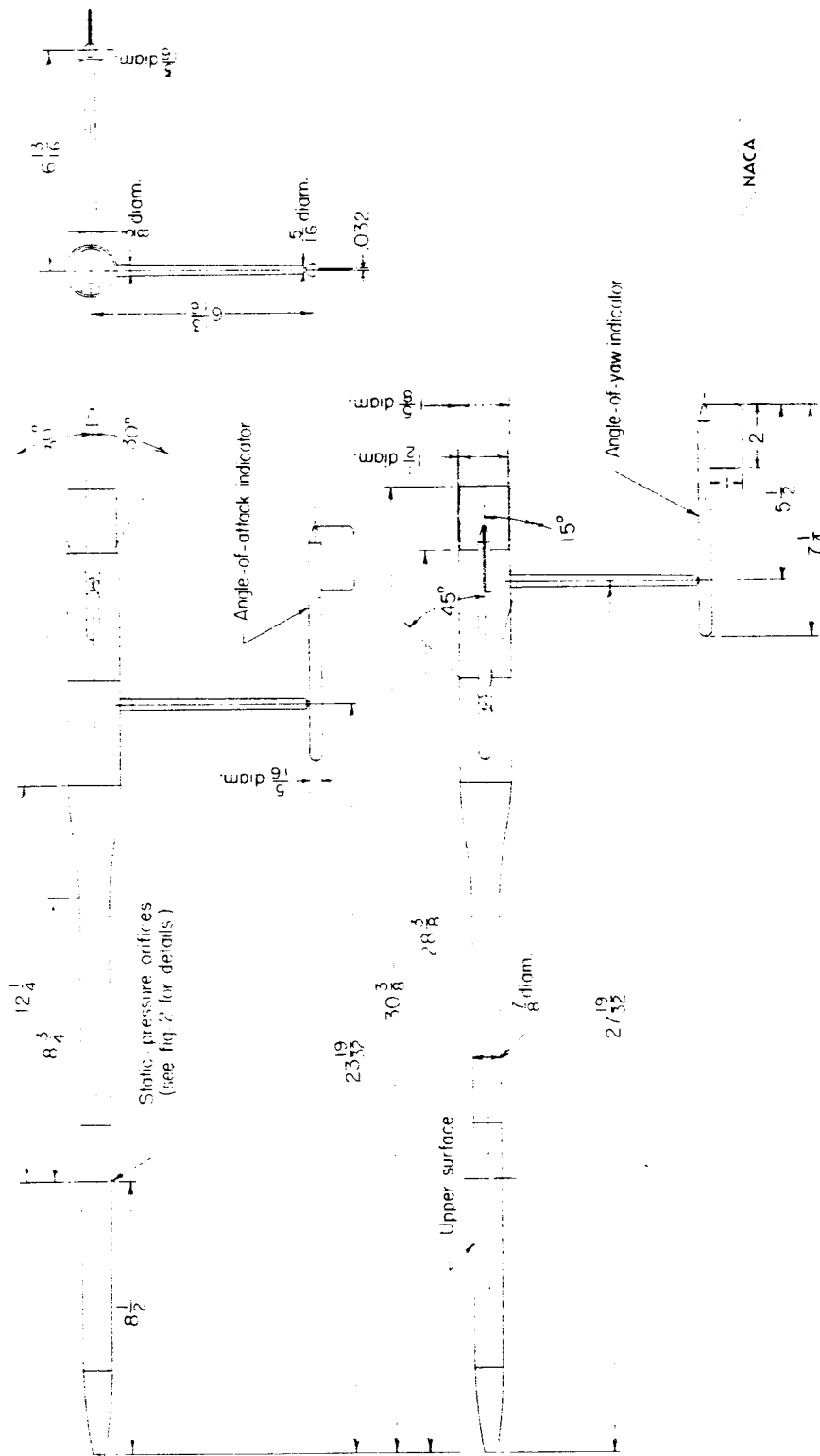


Figure 1.- Details of combination pitot-static tube and vane-type flow-angularity indicator. All linear dimensions are in inches.

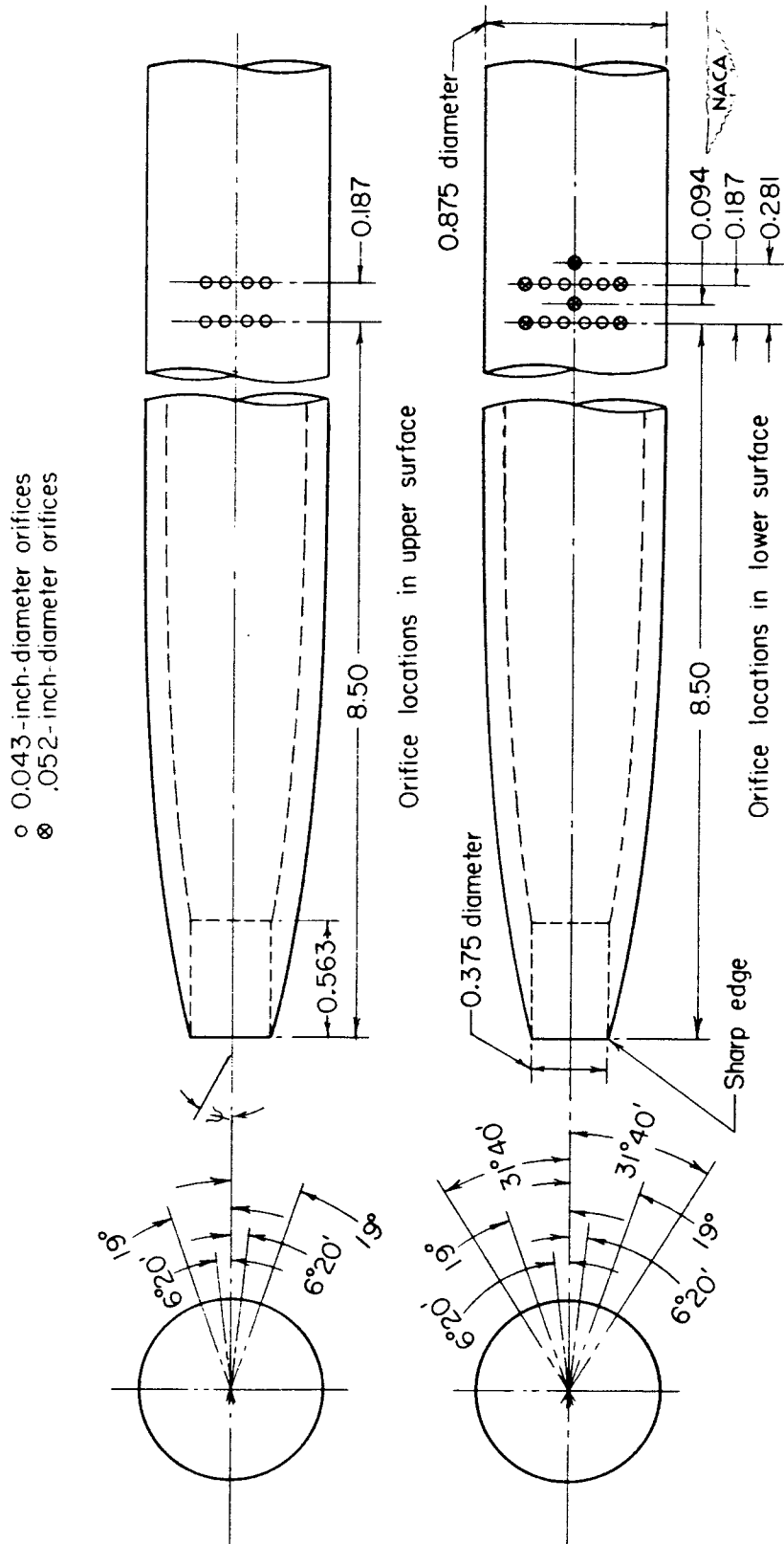


Figure 2.- Details of static- and total-pressure orifices. All linear dimensions are in inches.

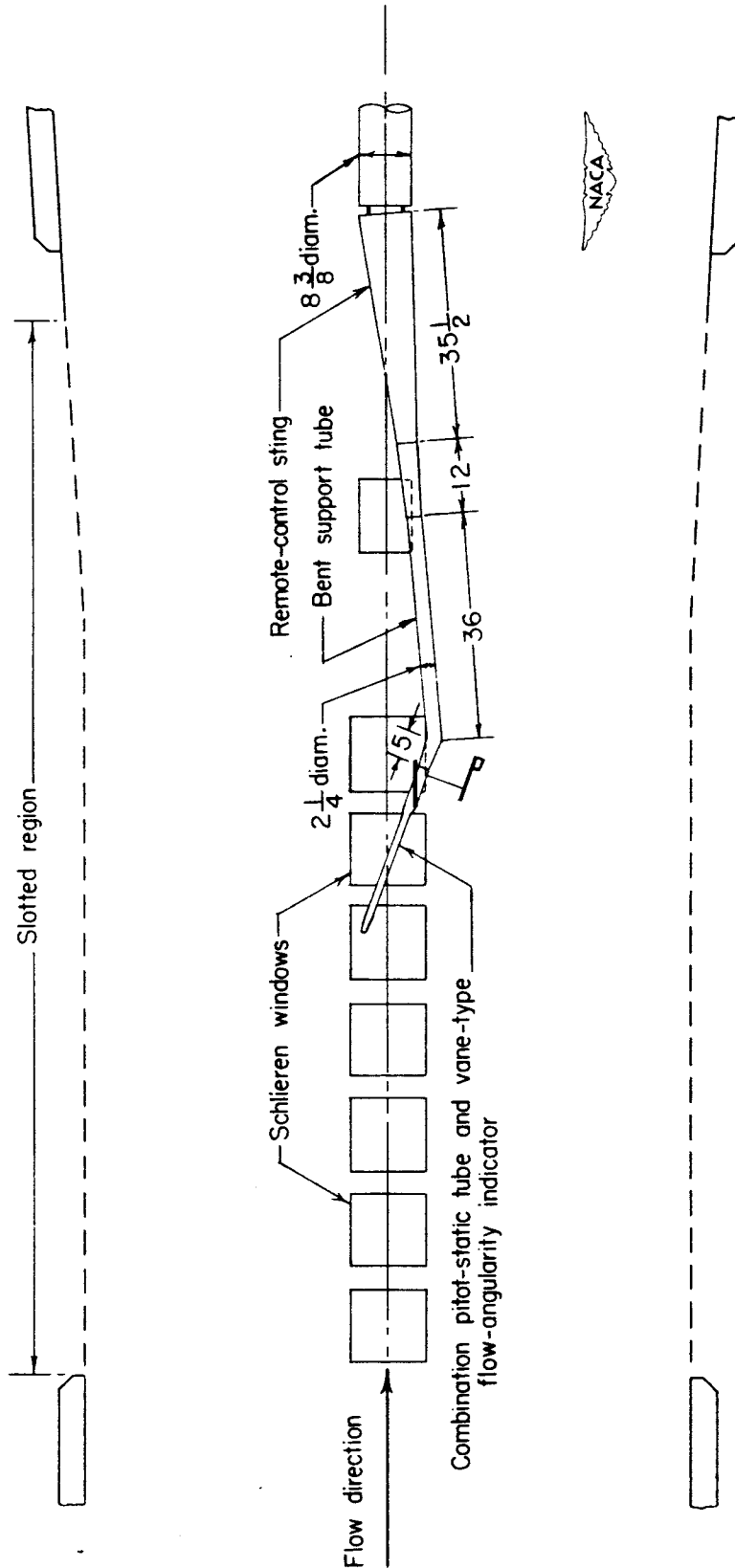


Figure 3.- Method of mounting the instrument in the Langley 8-foot transonic tunnel. Instrument shown at  $\alpha = 20^\circ$ ,  $\psi = 0^\circ$ . All dimensions are in inches.

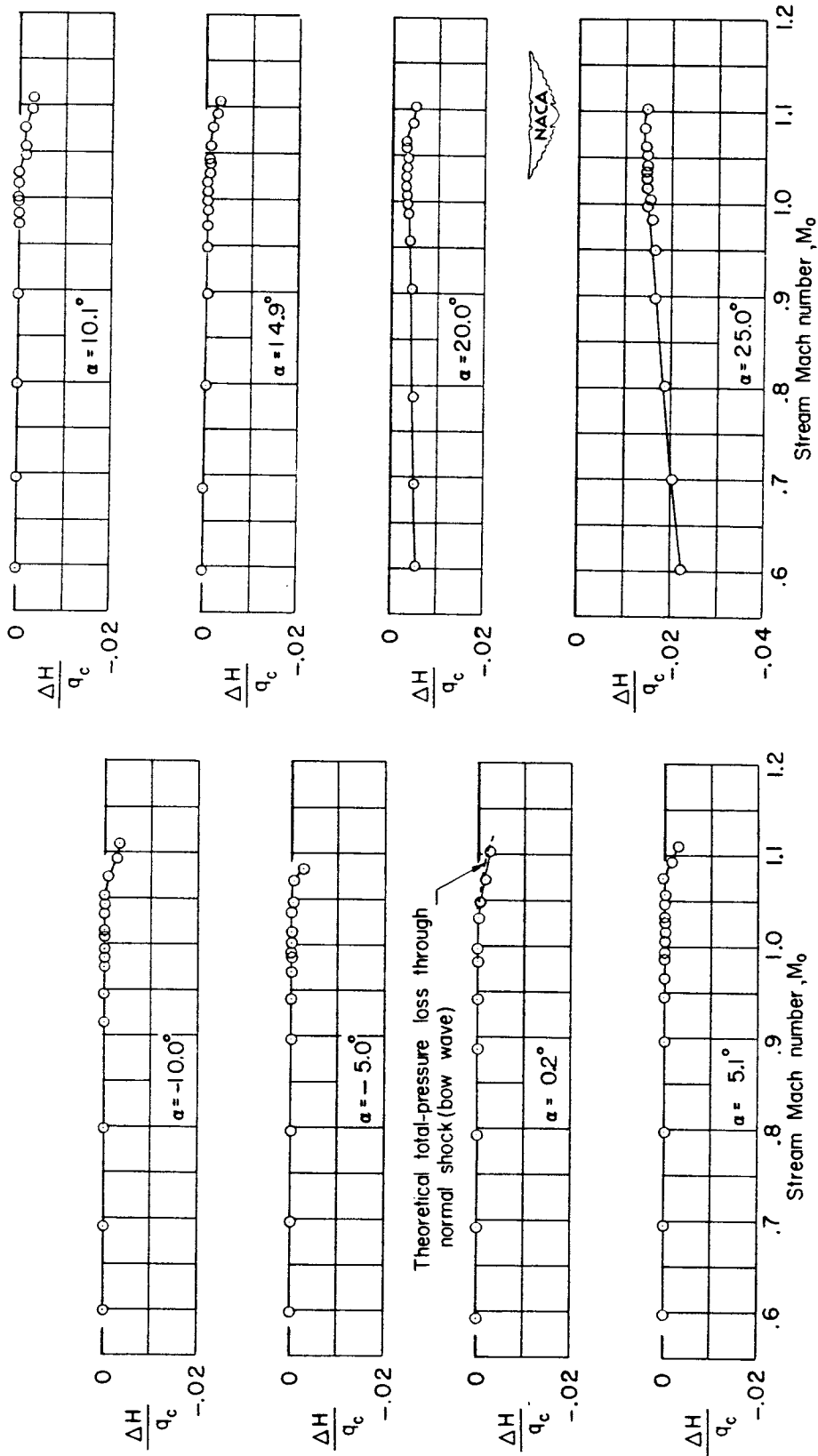


Figure 4.- Variation of total-pressure error with Mach number.  $\psi = 0^\circ$ .

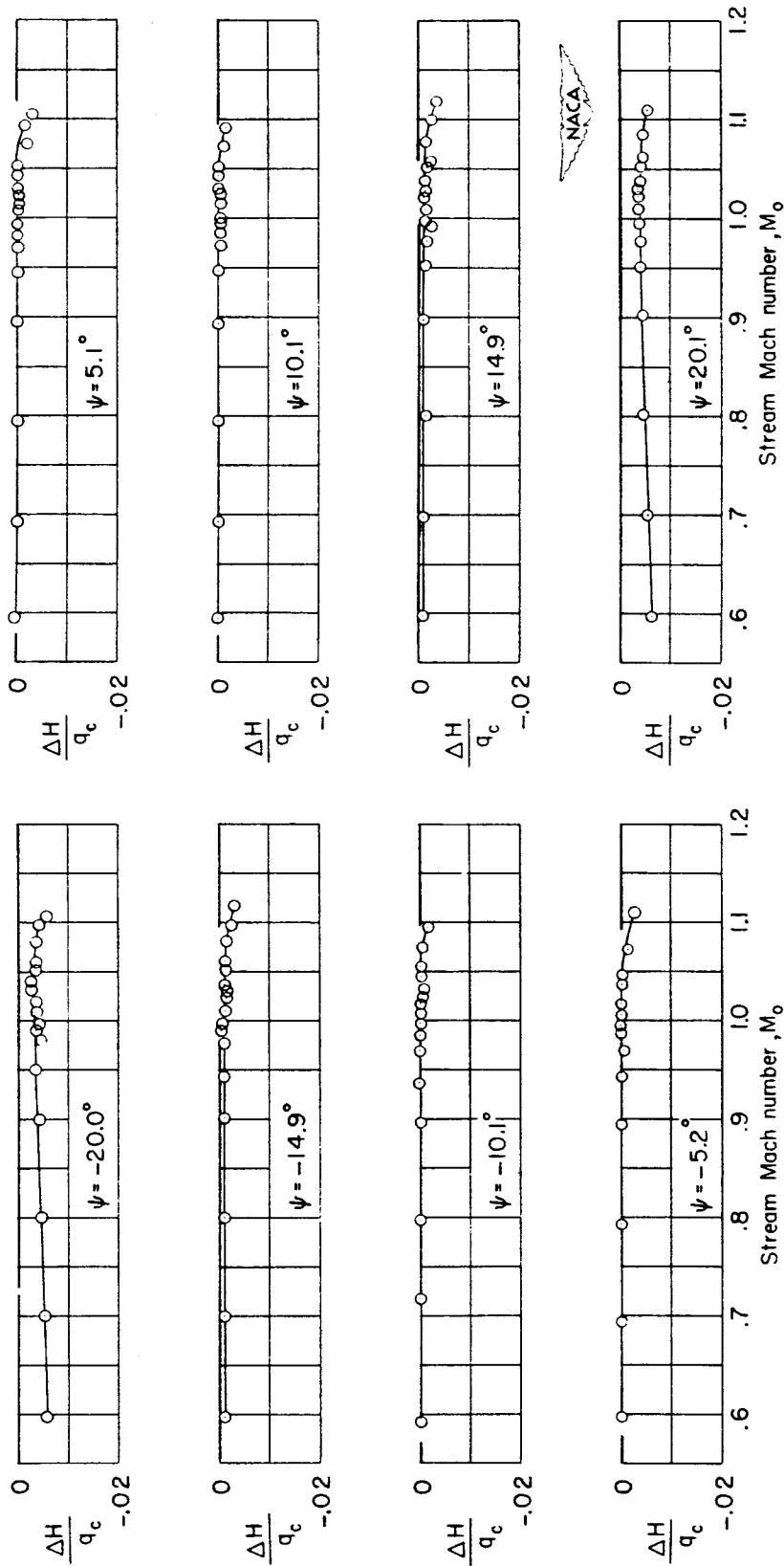


Figure 5.- Variation of total-pressure error with Mach number.  $\alpha = 0^\circ$ .

--- Corrected for total-pressure loss through a normal shock

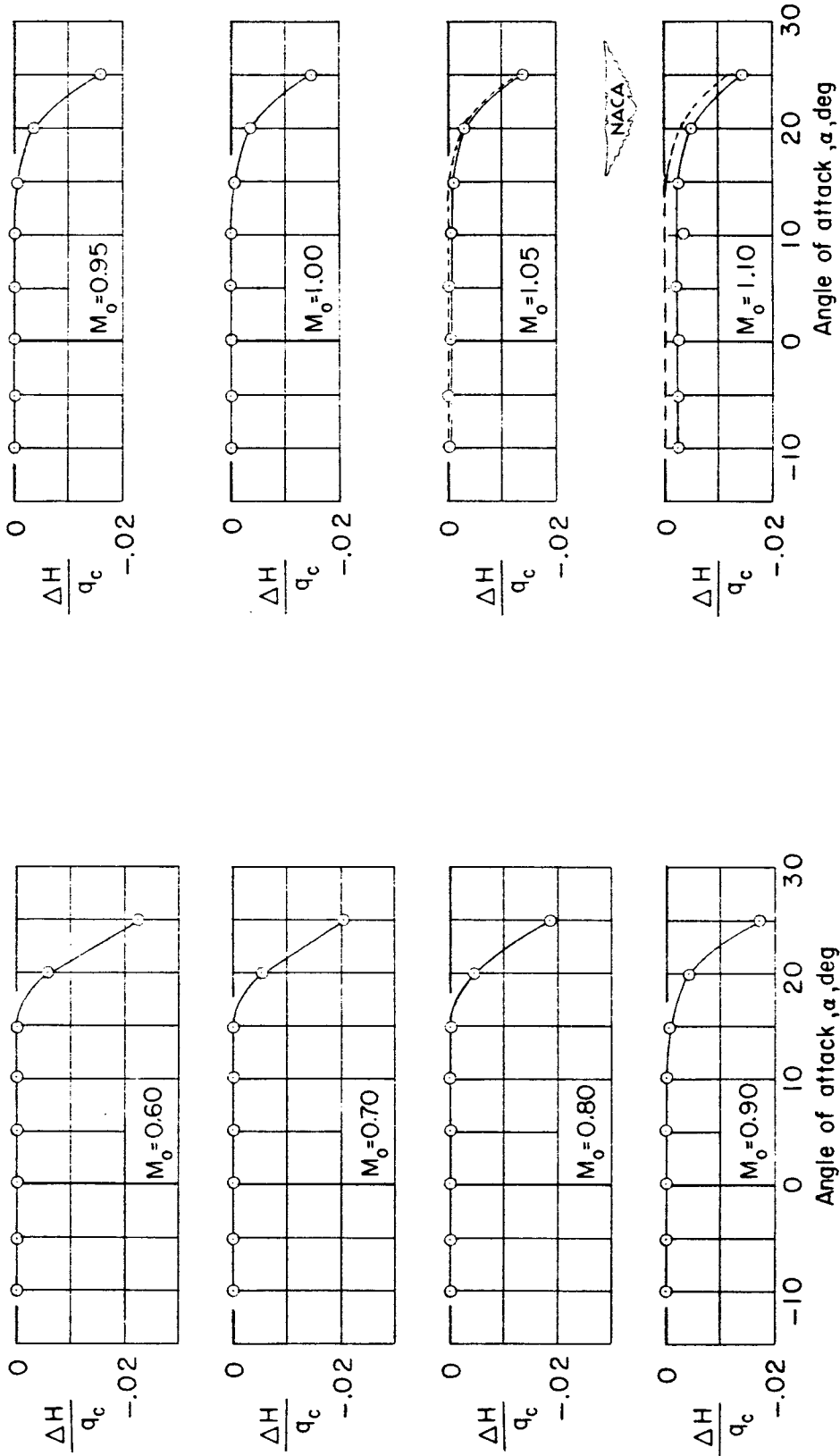


Figure 6.- Variation of total-pressure error with angle of attack.  
 $\psi = 0^\circ$ .



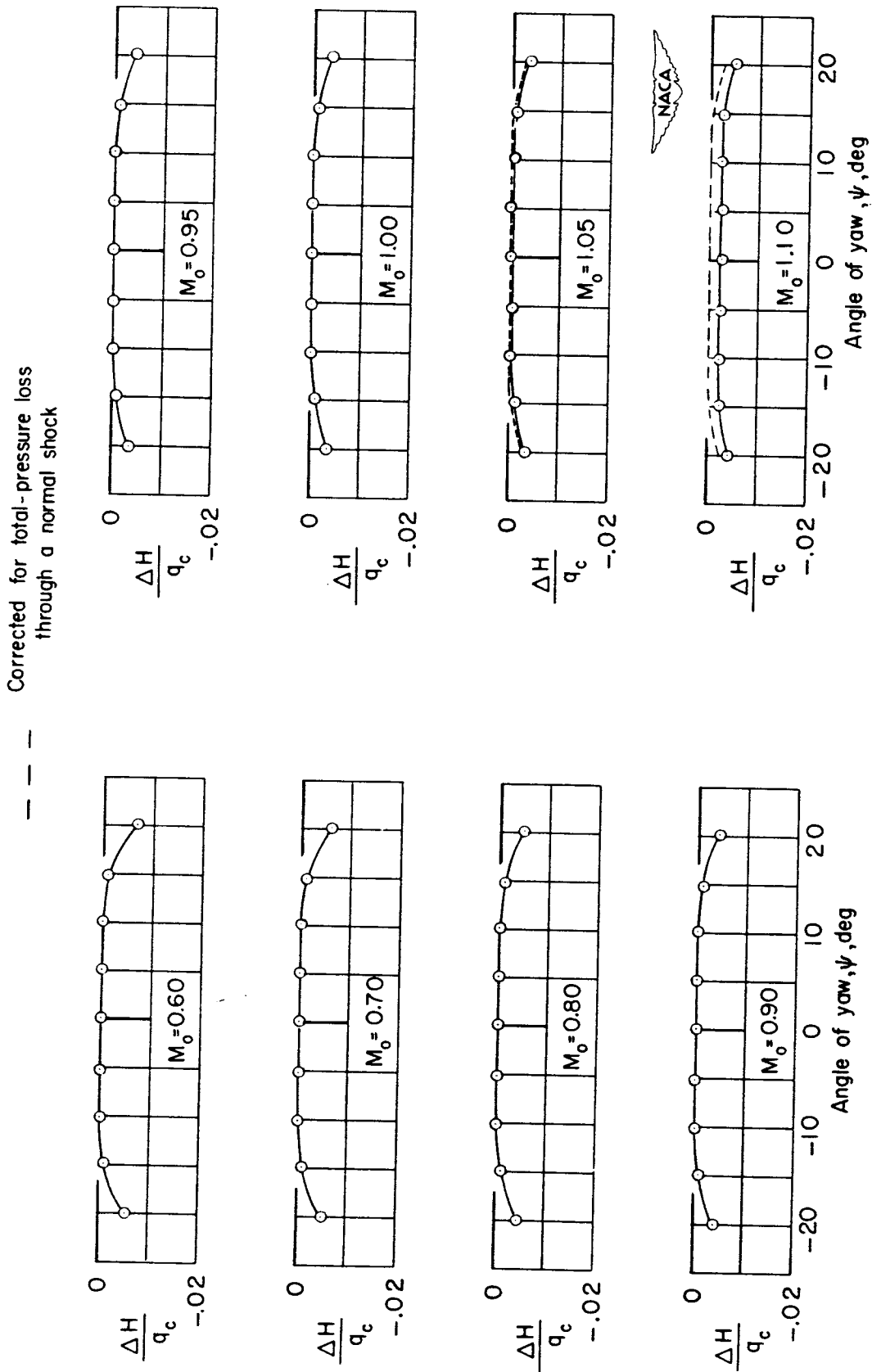


Figure 7.- Variation of total-pressure error with angle of yaw.  $\alpha = 0^\circ$ .

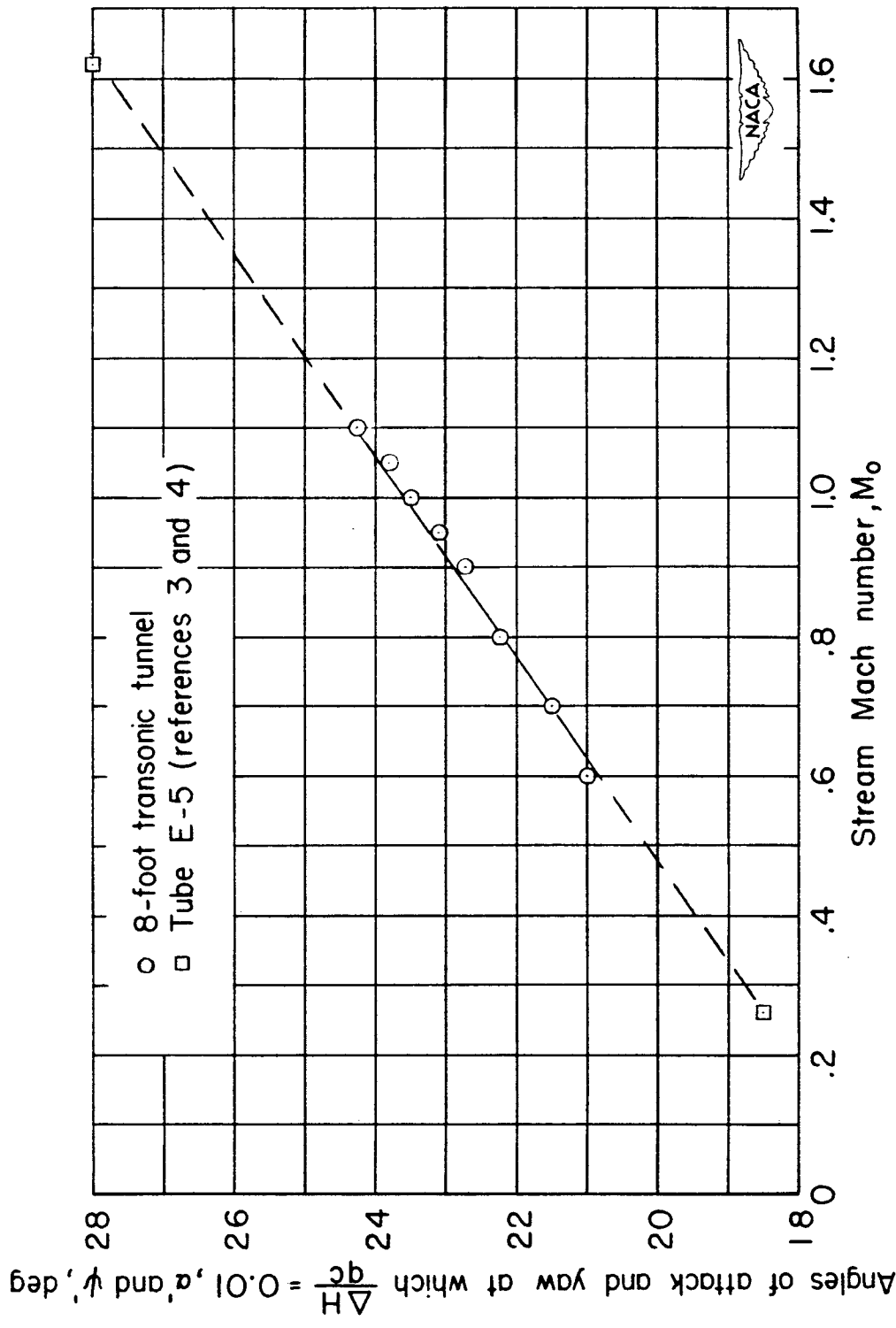


Figure 8.- Variation with Mach number of angles of attack and yaw at

which  $\frac{\Delta H}{qc} = 0.01.$

- a Compression due to tube enlargement downstream of static-pressure orifices
- b Overexpansion due to boundary-reflected disturbances
- c Compression due to boundary-reflected disturbances
- d Compression due to disturbance originating at boundary (not compensated for in tunnel-flow calibrations)

--- Estimated fairing

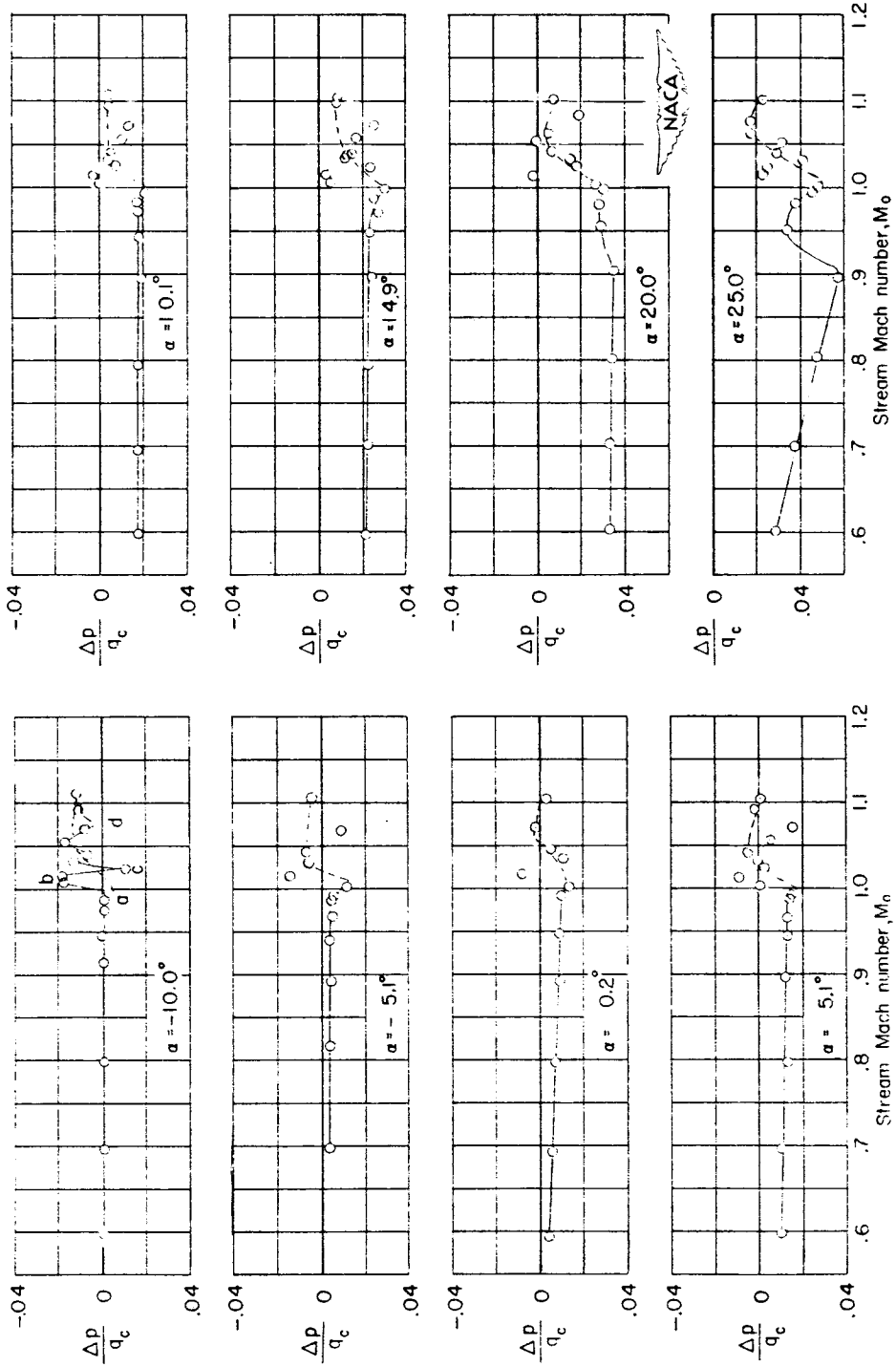


Figure 9.- Variation of static-pressure error with Mach number.  $\psi = 0^\circ$ .

- a Compression due to tube enlargement downstream of static-pressure orifices
- b Overexpansion due to boundary-reflected disturbances
- c Compression due to boundary-reflected disturbances
- d Compression due to disturbance originating at boundary (not compensated for in tunnel-flow calibrations)

--- Estimated fairing

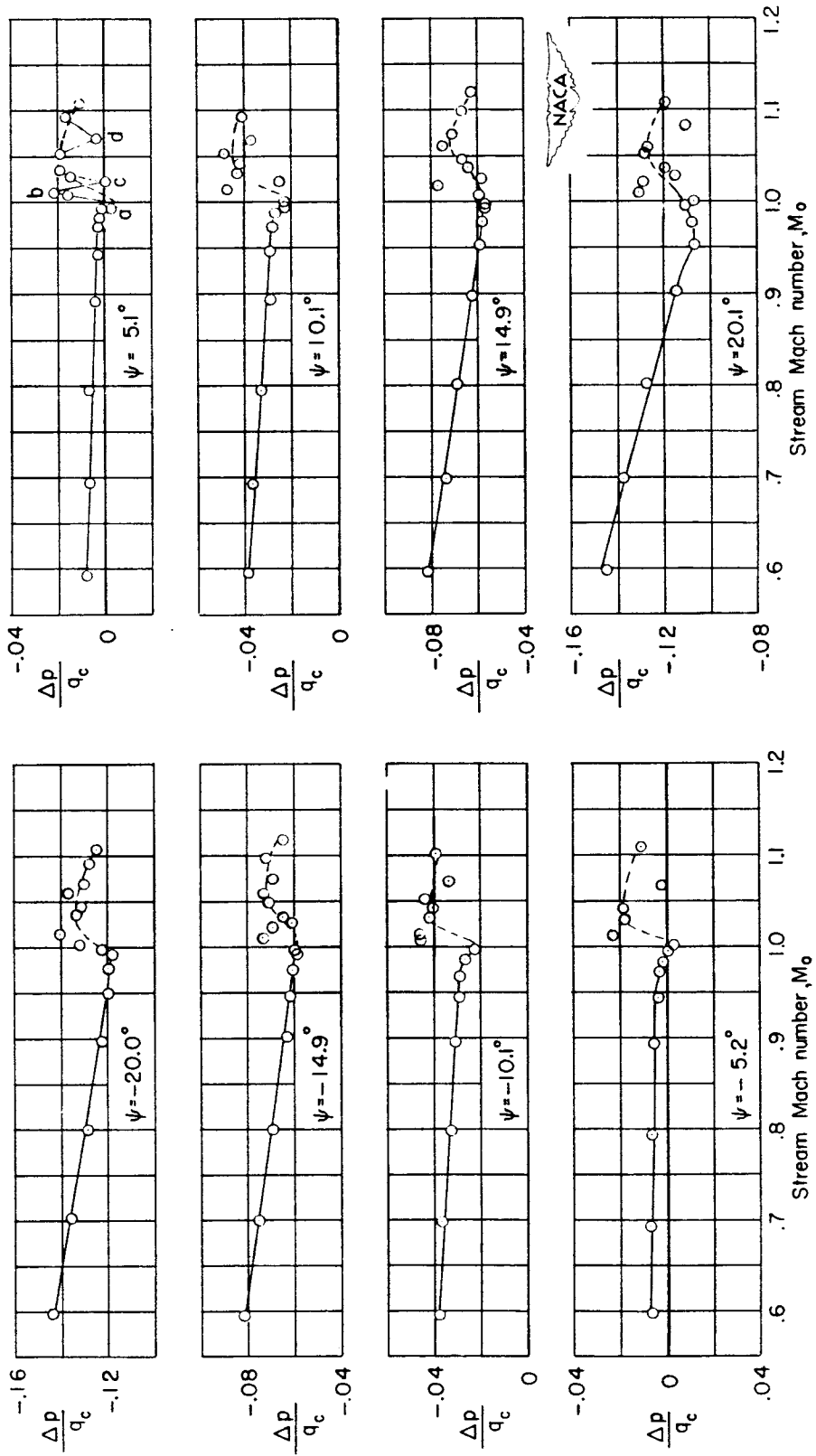
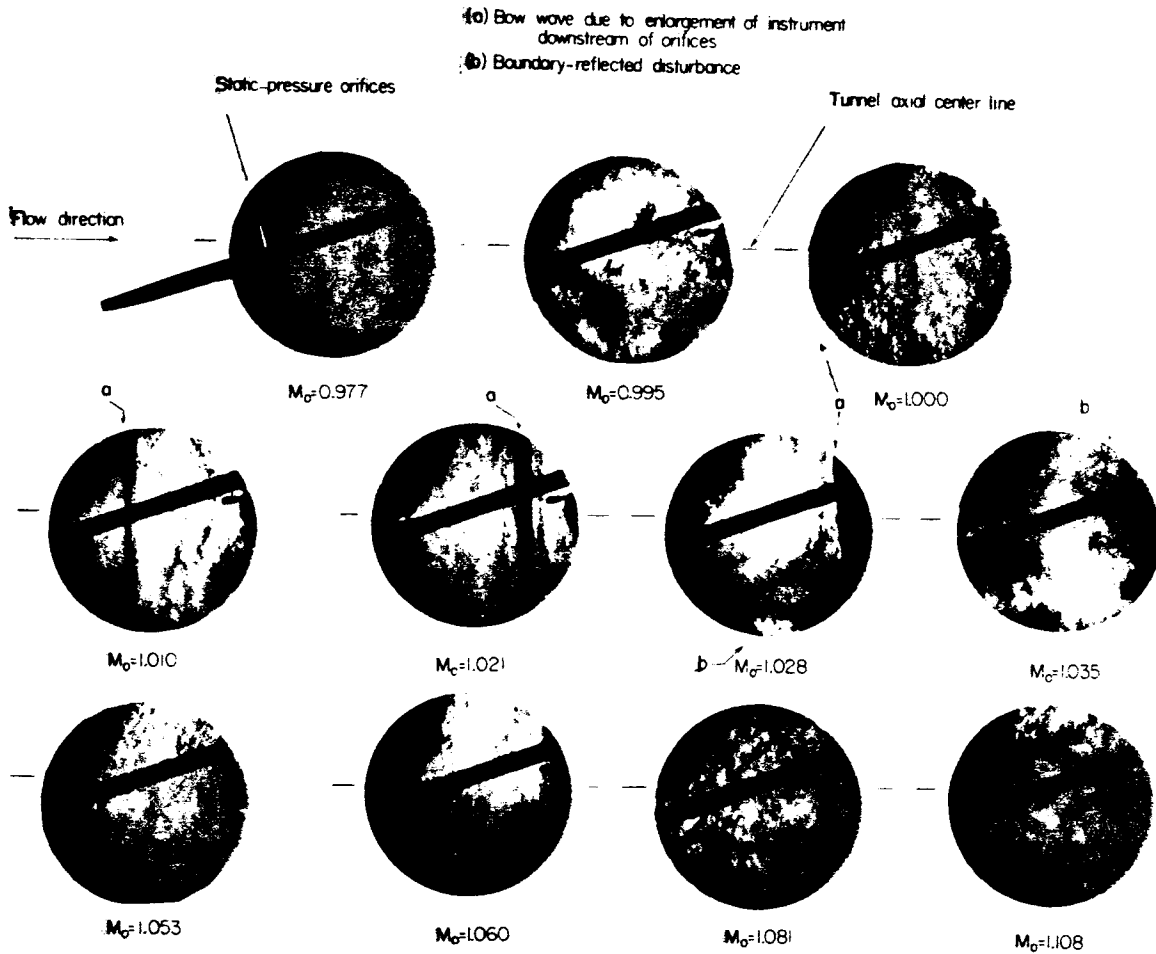


Figure 10.- Variation of static-pressure error with Mach number.  $\alpha = 0^\circ$ .



NACA  
 L-751143

Figure 11.- Shock formations and reflections at transonic speeds.  
 $\alpha = 0^\circ$ ;  $\psi = 20^\circ$ .

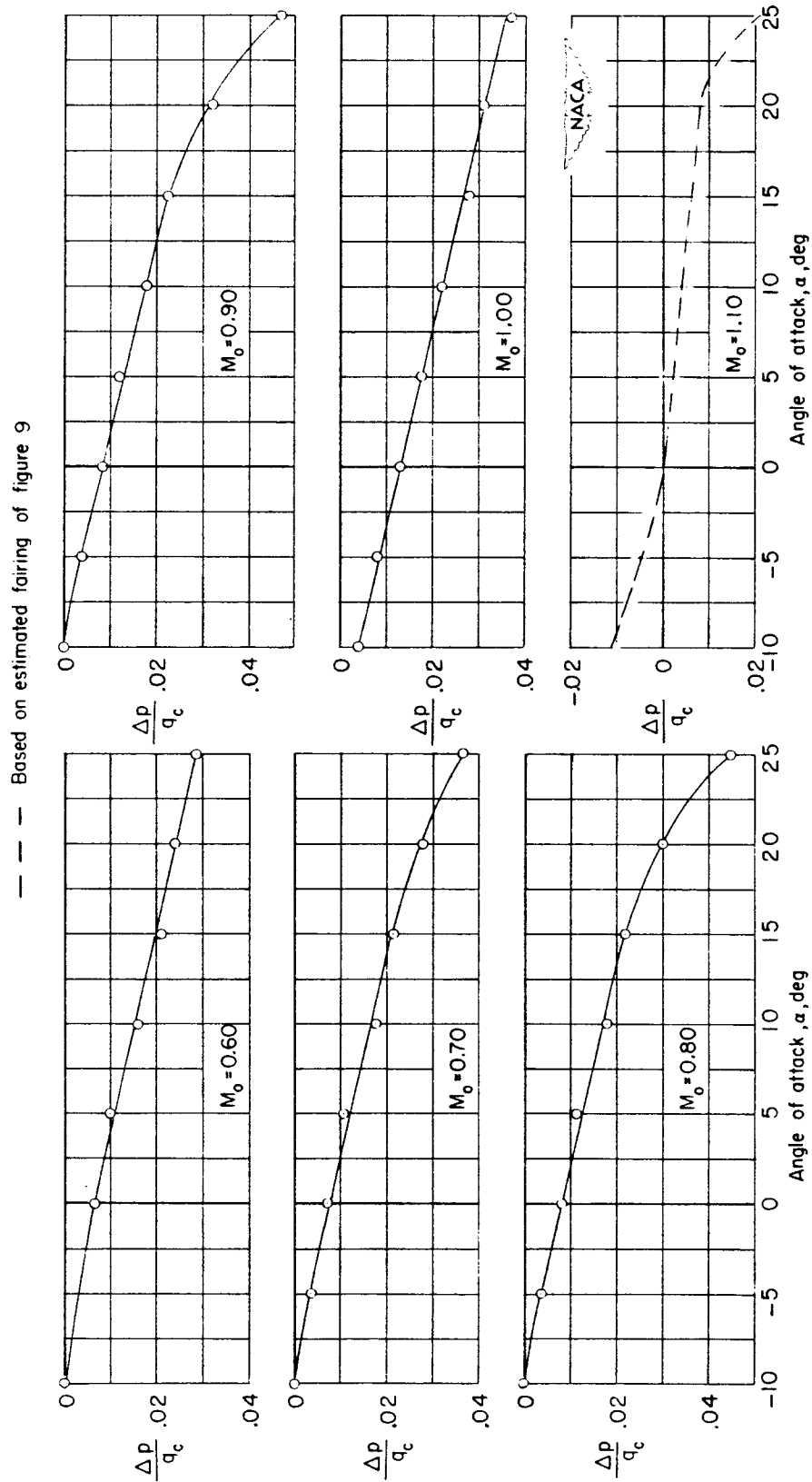


Figure 12.- Variation of static-pressure error with angle of attack.  
 $\psi = 0^\circ$ .

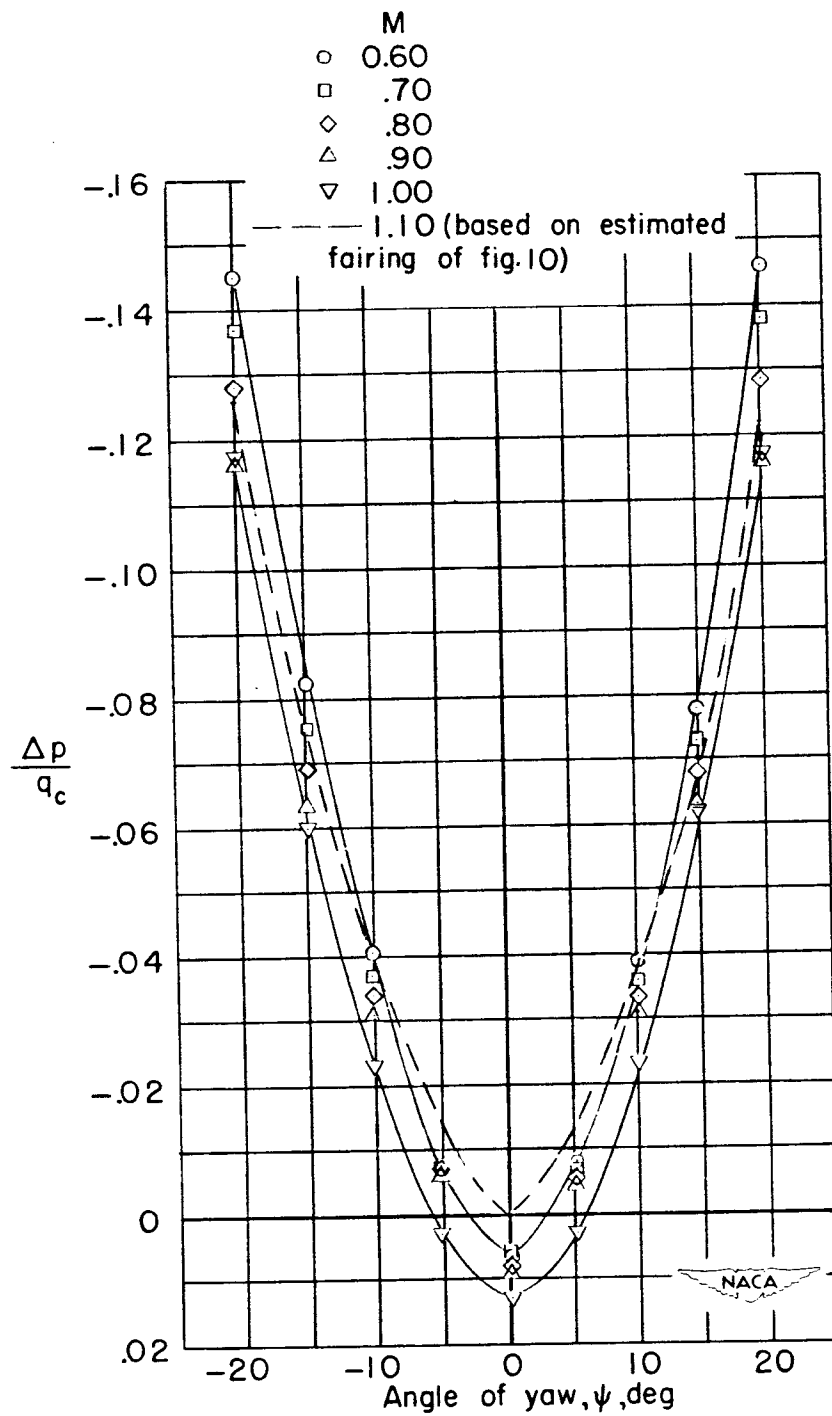
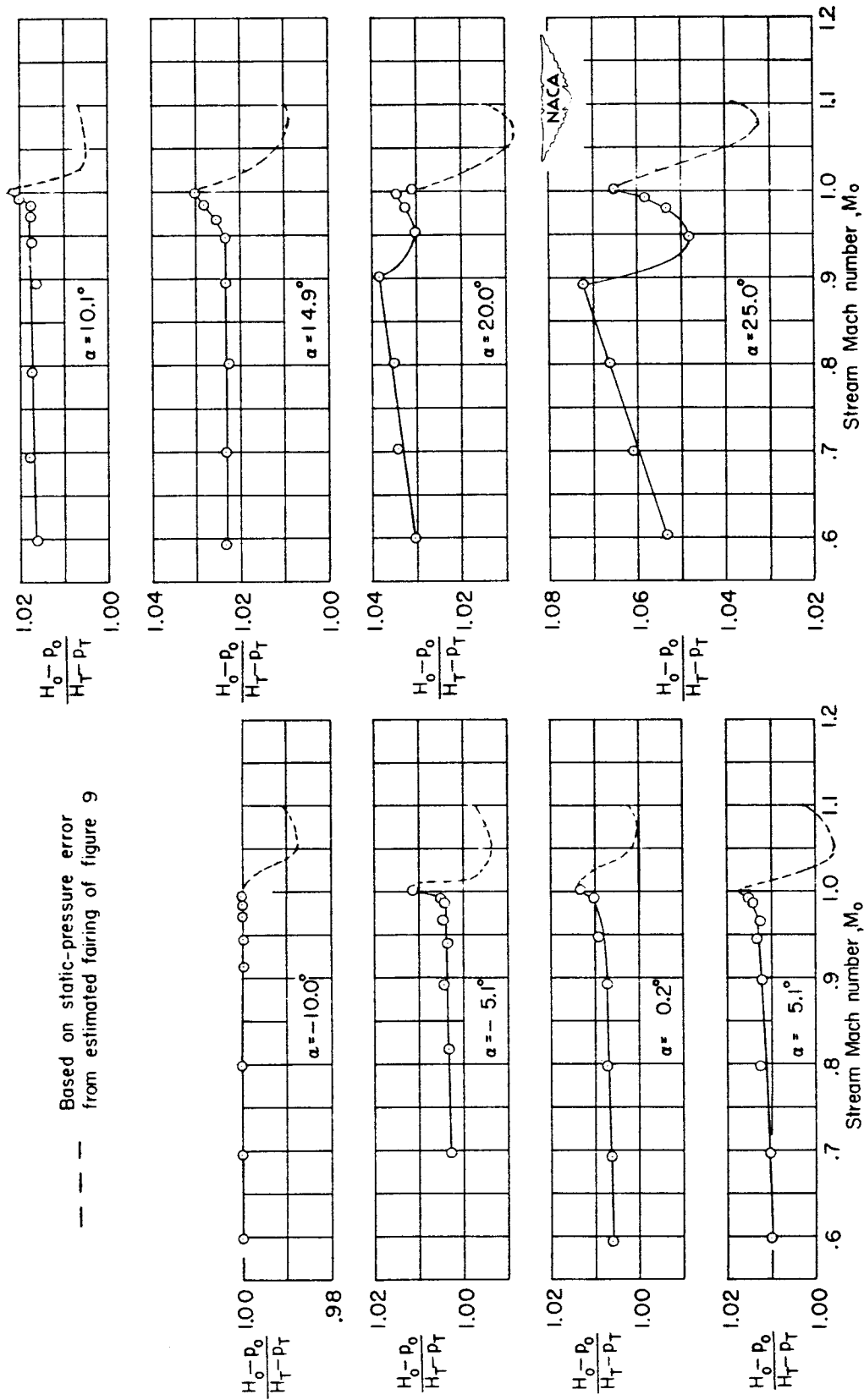


Figure 13.- Variation of static-pressure error with angle of yaw.  
 $\alpha = 0^\circ$ .



--- Based on static-pressure error  
from estimated fairing of figure 9

Figure 14.- Variation of calibration factor with Mach number.  $\psi = 0^\circ$ .



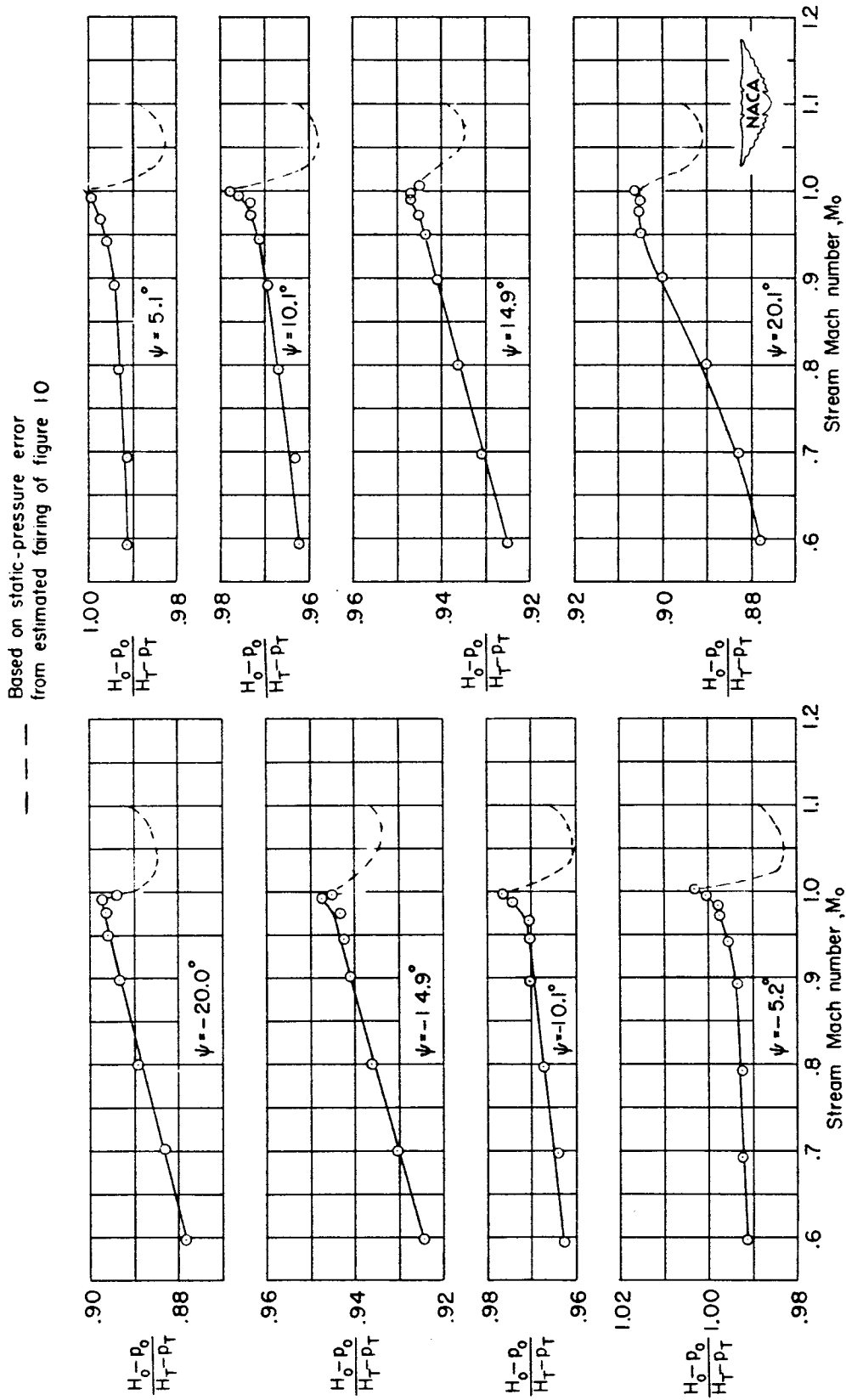
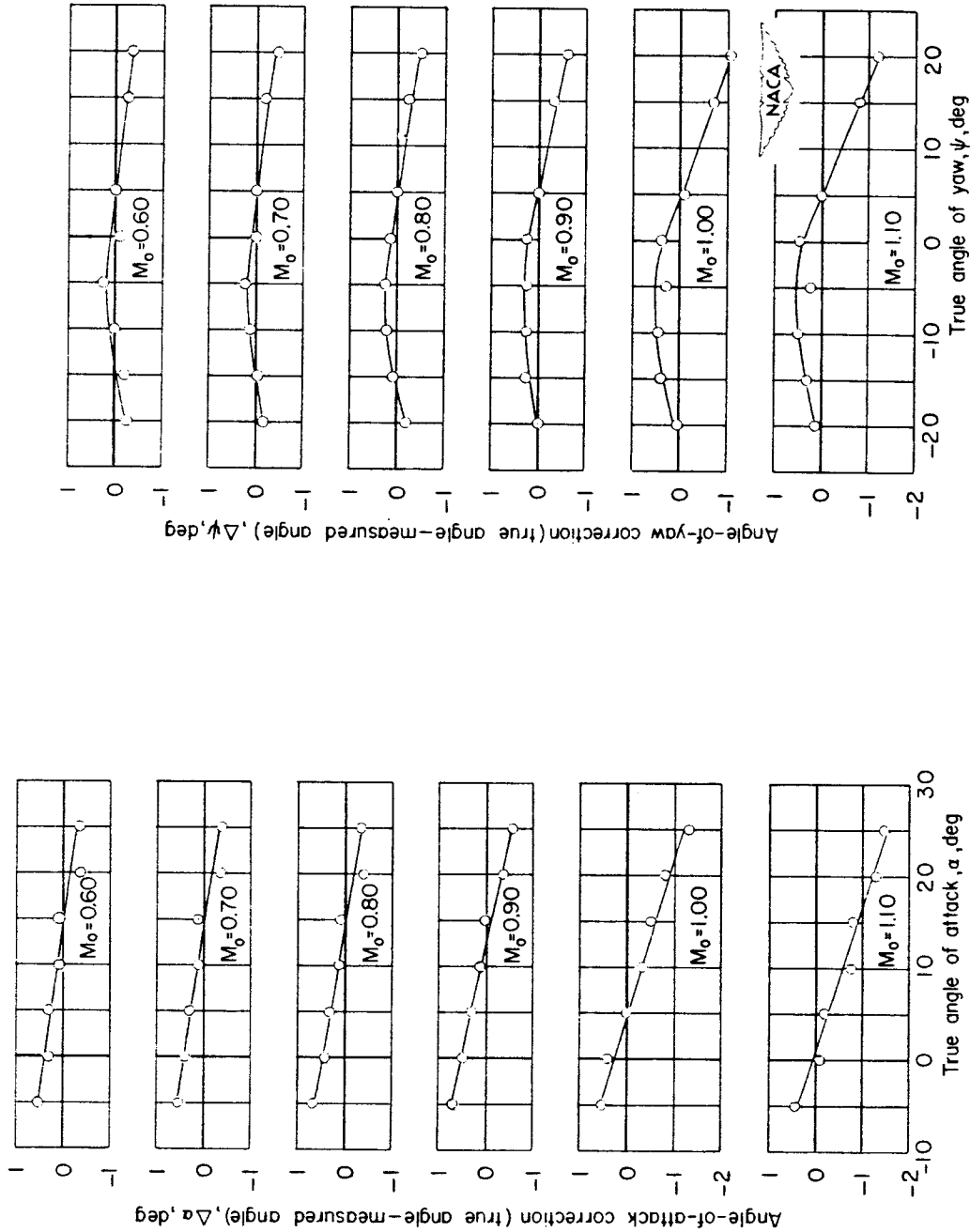


Figure 15.- Variation of calibration factor with Mach number.  $\alpha = 0^\circ$ .



(a)  $\psi = 0^\circ$ .

(b)  $\alpha = 0^\circ$ .

Figure 16.- Corrections for vane-type flow-angularity indication.